Environmental Technology & Innovation 32 (2023) 103286

Contents lists available at ScienceDirect

Environmental Technology & Innovation

journal homepage: www.elsevier.com/locate/eti

Electrochemical remediation of phenol contaminated kaolin under low-strength electric fields

Federica Proietto *, Abdo Khalil, Wissam Maouch, Alessandro Galia, Onofrio Scialdone

Laboratorio di Tecnologie Chimiche ed Elettrochimiche, Dipartimento di Ingegneria, Università degli Studi di Palermo, Viale delle Scienze, Ed. 6 , Palermo 90128, Italy

ARTICLE INFO

Article history:
Received 26 May 2023
Received in revised form 8 July 2023
Accepted 9 July 2023
Available online 13 July 2023

Keywords:
Electrochemical remediation
Electrokinetic
Electrochemical geo-oxidation
Kaolin remediation
Phenol
Low electric field

ABSTRACT

Soil degradation is a global concern. Electrochemical remediation (ER) technology is considered an appealing strategy for soil remediation because it is a low-cost, adaptable, and effective noninvasive *in situ* technology. Currently, the remediation of soil characterized by fine grains, low-hydraulic permeability, heterogeneous conditions, and mixtures of contaminants is still challenging since other conventional technologies are poorly effective. ER of soil is based on the application of low potentials between a couple of electrodes which induces an electric field (E) in the contaminated field. In this work, very low values of electric field ($E \leq 0.25$ V cm^{-1}) were used for the ER of contaminated kaolin. Phenol was selected as model hazardous organic compound and kaolin as model, reproducible and low buffering and low permeability clay. The effect of several factors, including the nature of the electrodes, treatment time, kind of current, the strength of the E and the nature of supporting electrolyte, on the performance of the process was investigated in detail and discussed in terms of the normalized phenol concentration and its total removal from the kaolin. Overall, the main finding is that the use of very low value of E (0.15 V cm^{-1}) can allow to simultaneously desorb, mobilize and also in-situ degrade phenol. The highest removals of phenol up to approximately 80% and 90% from the kaolin under both direct and sinusoidal E, respectively, were reached using compact graphite as electrodes in presence of Na_2SO_4 into the kaolin.

1. Introduction

Over the last century, lands and soils have been polluted by a wide range of industrial activities, which have discharged toxic chemicals into the environments. Both outcomes of accidental spills and improper management resulted in the presence of many contaminated sites worldwide (Chen et al., 2018; Gereslassie et al., 2019; Huysegoms and Cappuyns, 2017; Ronchi et al., 2019; Song et al., 2018a). Contaminants include a wide range of toxic pollutants such as polycyclic aromatic hydrocarbons, phenolic compounds, heavy metals, and radionuclides. Phenol and, more in general, phenolic compounds are typical organic pollutants found in soil and are considered as priority pollutants since they are dangerous for human health and ecosystem because of their recalcitrant nature and their toxicity (Annamalai et al., 2022; Karim et al., 2021; Lin et al., 2021; Vaiano et al., 2018; Thepsithar and Roberts, 2006). Soil degradation is a global concern and, to protect public health and the environmental, on 17 November 2021, the European Union Commission has adopted a new

* Corresponding author.
E-mail address: federica.proietto@unipa.it (F. Proietto).

https://doi.org/10.1016/j.eti.2023.103286

ambitious *EU soil strategy for 2030*. This program sets out a framework and concrete actions by 2030 to protect and restore soils, remediate contaminated sites, and ensure that they are used sustainably, to achieve healthy soils by 2050 (EU, Soil strategy for 2030, 2023). Currently, many conventional technologies are not effective or cheap for the remediation of sites characterized by fine grains, low hydraulic permeability, heterogeneous conditions, and mixtures of contaminants. The remediation of these sites has become a crucial priority. To face with this challenge, in the last years, several technologies based on physicochemical, thermal, electrochemical, and biological principles have been investigated (Annamalai et al., 2022; Sharma and Reddy, 2004; Vaiano et al., 2018). Among these approaches, electrochemical technologies have shown a great potential to remediate such complex polluted sites (Reddy and Cameselle, 2009). Electrochemical treatments could decrease soil contamination by transporting and/or transforming pollutants or extracting trapped materials (i.e., heavy metals, oils and petroleum) which may not be effectively recovered by other means. Over other conventional technologies, electrochemical remediation have shown unique advantages (Acar and Alshawabkeh, 1993; Reddy and Cameselle, 2009; Zanko et al., 2020) such as: (*i*) possibility to use it as both *ex situ* or *in situ* method; (*ii*) simple design and implementation on the field; (*iii*) easy integration with conventional technologies, including barrier and treatment systems; (*iv*) low-cost and efficient noninvasive technology; moreover, (*v*) it is practicable and adaptable for different kinds of contaminant and soils, especially for low permeability clayey deposits containing soluble and/or adsorbed compounds (Saini et al., 2021).

The electrochemical remediation (ER) of contaminated soil process is based on the application of proper potentials between a couple of electrodes which induces an electric field (E) in the contaminated field. Under the induced E, the process involves the movement of water (electroosmosis), ions (electromigration) and charged particles (electrophoresis) and electrochemical reactions (Acar and Alshawabkeh, 1993; Reddy and Cameselle, 2009; Zanko et al., 2020). According to the literature, the efficiency of the electrochemical treatment for the soil remediation depends on several factors including intensity and type of the applied E, soil pH, treatment time, nature of the electrodes, usage of enhancing agents (surfactants and chelating, oxidant agents (Tang et al., 2021; Wang and Wang, 2018)), contaminated media characteristics (such as buffer capacity, mineralogy, and organic matter content) among others (Reddy and Cameselle, 2009; Sharma and Reddy, 2004). Depending on the intensity of the applied E, the current literature commonly refers to electrokinetic (EK) processes ($E \geq 1$ V cm^{-1}) and electrochemical geo-oxidation (ECGO) processes (approximately $0.0025 < E < 0.25$ V cm^{-1}) (Reddy and Cameselle, 2009). However, in this last case, also the term EK at low potentials or EK under low-strength electric field is used. In the case of ECGO process it was reported that, other than the four principal mechanisms of electrolysis, electroosmosis, electromigration, and electrophoresis involved in the EK process (Acar et al., 1995; Tang et al., 2021; Wang and Wang, 2018), one more mechanism of electrochemical degradation was claimed, consisting in reduction–oxidation reactions at the microscale (Acar and Alshawabkeh, 1993; Saini et al., 2021; Zanko et al., 2020). Indeed, according to Rahner et al. (2002) and Röhrs et al. (2002), in this technology, the soil particles act as 'micro-conductors' and the wet soil as a 'diluted' electro-chemical solid bed reactor, in which electrochemical reactions can be induced on or near soil particles. This approach uses low voltage and/or both direct and alternating amperage applied in a proper sequence to induce reduction–oxidation reactions on soil solid surfaces at the micro-scale. According to previous literature, each sediment particle acts as a micro-capacitor that charges and discharges in a cyclic fashion; the energy burst on discharge at the micro-scale is intense, theoretically resulting in transformation of most organic contaminants to CO_2 and H_2O near the conducting particle surface (Sharma and Reddy, 2004; Zanko et al., 2020). ECGO self-generates the agents for reduction (H as ion or radical) and oxidation (O elemental, OH and its radicals, HO_2 and its radicals) at the electrode sites as well as within the pores. Hence, two kinds of electrodes can be observed in EK under low-strength electric field technology: (*i*) working electrodes to induce the electric field into the soil and (*ii*) the soil particles serving as microelectrodes including the solid/electrolyte interface (Sharma and Reddy, 2004). This approach is especially appealing because there is no need to add external oxidants (Zanko et al., 2020). The mobility of organic pollutants in contaminated sites is usually poor, resulting in slow remediation processes. In the last years, the removal of phenol and more in general of phenolic compounds from the soil was investigated by few authors (Acar et al., 1992; Luo et al., 2005, 2006; Thepsithar and Roberts, 2006; Zhang et al., 2005). Most of the works were performed under a $E \geq 1$ V cm^{-1} with the aim to mobilize and transport the compounds from the soil towards the electrolyte compartments (Acar et al., 1992; Luo et al., 2005, 2006; Zhang et al., 2005). The common finding of these works was that the induced E could desorb and drive the phenol through the soil towards the electrode compartments generating a secondary pollution, which must be disposed of and treated as dangerous waste effluent. In addition, post-treatment of the extracted solutions at the electrodes makes this treatment very costly. In the current literature, ER approach under low-strength electric field (e.g. ECGO) was widely investigated coupled with other technologies, e.g. the phytoremediation of contaminated soil, resulting in a good process performances (Acosta-Santoyo et al., 2017). Up to our knowledge, the ER of soil and/or low permeability clay from organics using a low-strength electric field (i.e. less that 0.25 V cm^{-1}) was investigated at lab-scale, mainly mediated by microbial activity (Chen et al., 2021; Huang et al., 2011; Li et al., 2017; Wu et al., 2018). Zanko et al. (2020) reported the application of the ECGO technology for the treatment of sediments contaminated by polychlorinated biphenyls (PCBs) from New Bedford Harbor (NBH), Massachusetts, for approximately 1900 days. More recently, attempts were made to evaluate the treatment of metals using this process; Hsueh et al. (2022) investigated the possibility to treat Cr/Ni contaminated soil (sandy loam composed of 96.0% sand and 4.0% clay) by EK/ECGO system by varying several operating parameters, including the electrode configuration, potential gradient, processing fluid. In this framework, very low results on basic of the ECGO process at lab scale are reported in the literature. Hence, to investigate this technology, in this work, very low values of electric field ($E \leq 0.25$ V cm^{-1}) were used for the ER of contaminated kaolin at lab-scale. Phenol (200 mg/Kg) was selected

as model hazardous organic compounds due to its recalcitrant nature and toxicity, while kaolin was employed because it provides a model, reproducible and low-buffering clayey soil. Hence, the effect of several factors, including the nature of the electrodes (graphite, stainless steel, DSA®/Pt), treatment time (over 4-days), kind of current (direct or a sinusoidal E), the strength of the E and the nature of supporting electrolyte (NaCl, Na_2SO_4), on the performances of the process was investigated in detail and discussed in terms of the normalized phenol concentration (i.e. $C_{\text{Phenol}}/C^0_{Phenol}$ where C_{Phenol} and C^0_{Phenol} are the phenol concentration after the treatment and its initial one, respectively) and its total removal from the kaolin.

2. Materials and methods

2.1. Chemicals

Bi-distilled water and phenol (Merck, purity > 99%) were used as solvent and model pollutant, respectively, while NaCl (Sigma Aldrich, ≥ 99%, 0.1 M) and Na_2SO_4 (Sigma Aldrich, ≥ 99%, 0.1 M) as supporting electrolyte. Methylene chloride (Riedel-de Haën, puriss p.a., Reag. ACS, Reag ISO) was used to extract phenol from the kaolin samples. Acetonitrile and high-performance liquid chromatography (HPLC) grade water were obtained from Sigma Aldrich. All chemicals were at least ACS-grade and were used as received without further purification. Compact graphite (Carlo Erba Reagents), commercial stainless steel AISI 316, a Ti/IrO_2–Ta_2O_5 sheet (commercial DSA® –Dimensionally Stable Anodes, - which is a titanium anode coated with proprietary and patented mixed metal oxide compositions comprised of different elements, i.e., iridium and tantalum (Ti/IrO_2–Ta_2O_5 sheet) supplied by ElectroCell AB) and platinum plate (99.9% trace metals basis) were selected as electrodes material.

2.2. Spiked-kaolin and electrochemical remediation experiments

Kaolin, a hydrate aluminum silicate material, ($Al_2Si_2O_5(OH)_4$) was used as a model, reproducible, low-buffering, and low permeability clay mineral. For this work, kaolin is in the form of a fine white to light yellow powder (product specification CAS N:1332-58-7, supplied by Sigma-Aldrich) with a particle size distribution (when dry) of between 0.1 and 4 μm and naturally acid (using a water/kaolin mass ratio of 1.8: pH 3.78) (Al-Shahrani and Roberts, 2005). Before to be spiked, 100 g of kaolin pleaced in a Pyrex horizontal vessel and was dried for 24 h in an oven at 105 °C. After the kaolin was artificially spiked with phenol at 200 mg/Kg of dried kaolin reaching a water content, W, of approximately 66%. In particular, to prepare 100 g of spiked kaolin at W of 66%, 40 g of an aqueous solution of 3.2 mM of phenol was mixed with 60 g of dried kaolin, sealed and equilibrated for 24 h by using a horizontal shaker at 200 rpm. It is reported that the phenol adsorption capacity of the kaolin is 300 mg/Kg (Safwat et al., 2019). In our case, the initial content of phenol was less than the saturated sorption amount, thus letting us to assume that most of the phenol is absorbed at the kaolin at this content. The initial pH was approximately 6.

Electrolyses was conducted in a Plexiglass® electrokinetic cell of total empty volume of 60 mL. A pair of electrodes (active area of 3 cm^2) were symmetrically inserted into the clay bed and the distance between anode and cathode was 10 cm (System I, Fig. 1a). The moist spiked kaolin was then placed into the electrokinetic cell by layers. Each layer was pressed down using a Plexiglass pestle and vibrated so that the amount of void space was minimized. After that, the kaolin specimen was compacted for 12 h. 66 g of spiked and moist kaolin was inserted in System I. When 66 g of spiked kaolin was placed in the cell (filled volume of the cell, V = 40 cm^3), its water content, W, was approximately of 66%wt., bulk density, ρ_b, of 1.65 g cm^{-3}, a specific gravity, G_s, at 20 °C of 2.43 (determined according to ASTM D 854-02) and a porosity, ξ, of 0.59 ($\xi = Vv/V = (V - V_s)/V = 1 - (w_{\text{dried-kaolin}}/G_s\rho_w)$)/V, where v_v, v_s, $w_{\text{dried-kaolin}}$ and ρ_w were the void volume, solid volume, placed dried kaolin mass ($w_{\text{dried-kaolin}}$ = 39.6 g) and the water density (ρ_w = 0.997 g cm^{-3}) respectively).

Then, at zero time, kaolin samples were retained to determine the actual initial content of phenol (C^0_{Phenol}), kaolin pH, and water content (W), since a portion of the pollutants and water could volatilize during the preparation. Once the preparation was completed, the system I was enclosed with a Plexiglass cover to prevent the kaolin bed from excessive evaporation of water. A constant direct or sinusoidal electric field (E) was applied to the electrodes using an Amel 2053 potentiostat/galvanostat or a Philips PM 5134 function generator 1 mHz–20 MHz, respectively. The electric field gradient ranged from 0.005 to 0.25 V cm^{-1} in the different tests.

Fig. 1b shows the system II (EK) used to perform an electrokinetic treatment under high E value of 1 V cm^{-1}. System II was a home-made Plexiglass® cell. It is constituted by three compartments: two external electrolyte compartment (V = 30 mL) filled with deionized water where electrodes were located and one central compartment where the spiked kaolin is placed. In this case, a total amount of 100 g of spiked kaolin with a moisture of 66% was placed inside the cell. Two compact graphite electrode (area 4 cm^2) was used. The cell was sealed by using stainless steel bolts and leakage was avoided by using O-rings placed among the different section. Filter paper was used to avoid that the clay particles was mixed with the electrolyte compartments. Once the spiked kaolin was completed, system II was enclosed with a Plexiglass cover to prevent the kaolin bed from evaporation of water. In this case, an AMEL potentiostats/galvanostat Model 2549 was used.

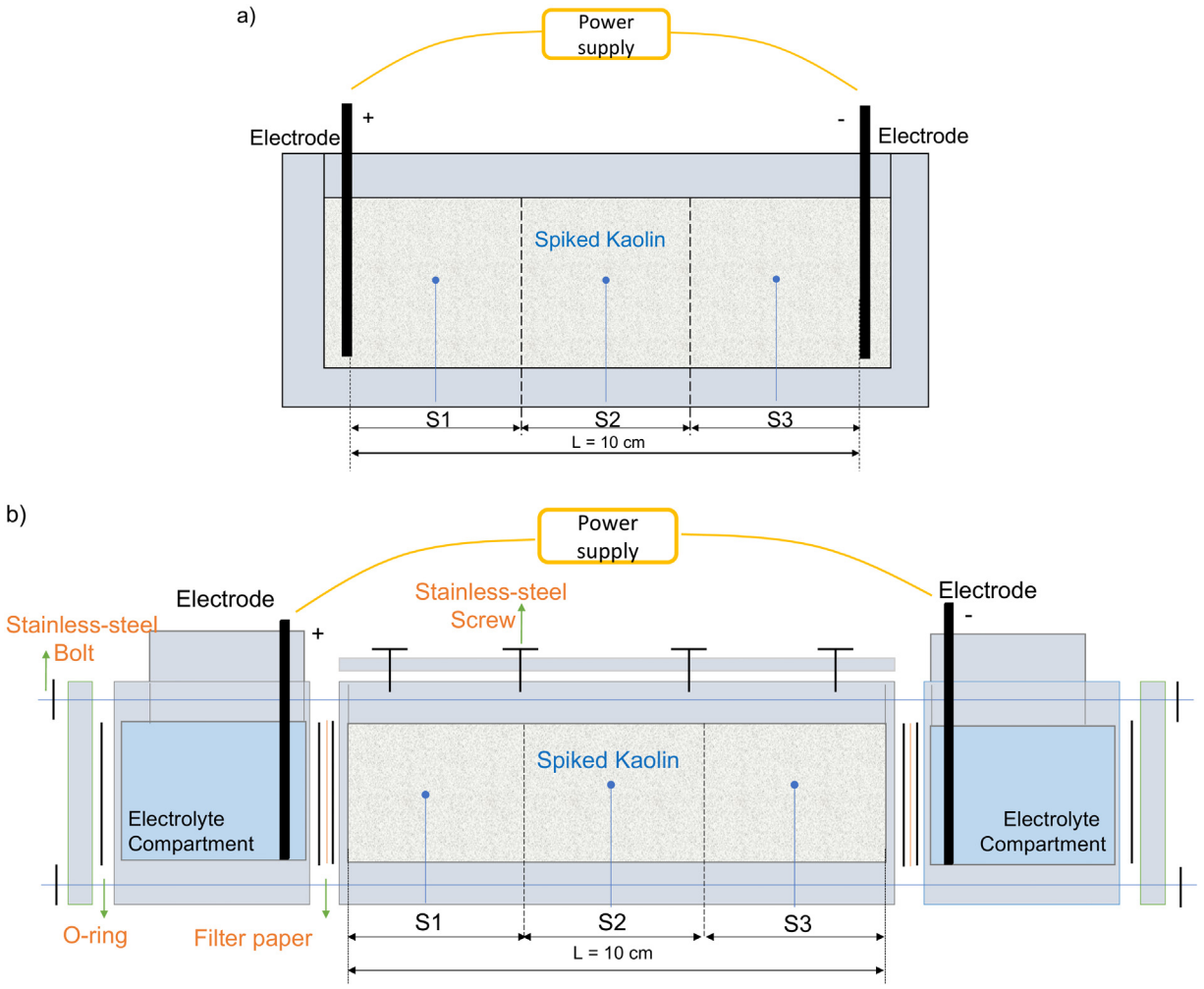

Fig. 1. Schematic view of the electrochemical cell for the treatment of the spiked kaolin: (a) System I for treatment under low-values *E* (ECGO) and (b) System II for the electrokinetic treatment at 1 V cm^{-1} (EK).

Electrochemical treatments were conducted twice for each test to ensure reproducibility of the data, and control experiments with no application of electric field were carried out. The experiments were conducted at ambient temperature over a 1-, 2- or 4-day period.

At the end of each electrochemical treatment, kaolin samples were taken to analyze the residual content of phenol in the kaolin, kaolin pH and water content. The sampling section are shown in Fig. 1, namely S1, S2 and S3 which are the sampling position near to the anode, middle and cathode, respectively.

2.3. Analytical methods

Phenol was extracted from the kaolin samples using pure methylene chloride (Sigma-Aldrich) (Luo et al., 2006). Approximately 1.0 ± 0.05 g of the well mixed treated clay sample was mixed with 6.5 g of methylene chloride in a Teflon-sealed glass vial, extracted by sonication for 30 min and centrifugated at 4000 rpm for 30 min. Each kaolin sample was extracted three times to ensure that the phenol was extracted completely. The supernatant was filtered through 0.45 μm Teflon membrane and analyzed by HPLC.

The concentrations of phenol and chlorophenols (2-chlorophenol, 4-chlorophenol, 2,4-dichlorophenol, 2,6-dichlorophenol, 2,4,6-trichlorophenol) were evaluated by HPLC using an Agilent 1260 fitted with a Kinetex 5 μm C18 column 100 Å 150 * 4.6 mm (Phenomenex) at 25 C° and coupled with a UV detector working at 214 nm. A solution of water (Honeywell, HPLC grade) and acetonitrile (Merck, HPLC grade) has flowed at 1 mL min^{-1} as the mobile phase into the column. It was used a gradient type of elution. In particular, the gradient profile was: (i) time = 0 min 20/80%vol/vol acetonitrile/water; (ii) time = 5 min 95/5%$_{vol/vol}$ acetonitrile/water. The detection limits were estimated based on the

standard deviation of the response and the slope of the calibration curve. According to the ICH guidelines, LOD = 3.3 σ/S and LOQ = 10 σ/S where σ is the standard deviation of the response calculated using the Microsoft Office Excel function "ERR.STD.YX" and S is the slope of the calibration curve. LOD and LOQ were estimated to be approximately 13 and 4 mg_{Phenol}/Kg, respectively. Calibration curves were obtained by using the pure standards of phenol (purity > 99%, Merck) (retention time 3.8 min), 2-chlorophenol (purity > 99%, Sigma-Aldrich) (retention time 4.6 min), 4-chlorophenol (purity > 99%, Sigma-Aldrich) (retention time 4.7 min), 2,4-dichlorophenol (purity > 99%, Sigma-Aldrich) (retention time 5.3 min), 2,6-dichlorophenol (retention time 5.15 min), (purity > 99%, Sigma-Aldrich), 2,4,6-trichlorophenol (purity > 99%, Alfa-Easer) (retention time 5.8 min) with respect to the methylene chloride (Riedel-de Haën, puriss p.a., Reag. ACS, Reag ISO). The aqueous electrolytes after treatment using System II were analyzed by HPLC equipped with the kineticx 5 μm C18 column (Phenomenex) with the same method to identify phenol, in this case the calibration curve was performed using different concentration of phenol solution.

The kaolin pH was measured with a Checker® pH Tester (HI98103) supplied by HANNA® instruments using a ratio kaolin:water of 1:10. Before the measurement of the pH, the sample was equilibrated for 6 h by using a horizontal shaker at 200 rpm.

Moisture, which represents the water content (W), was calculated according to the method NF P 94-050 (Eq. (1)):

$$W = \left(w_{evaporatedwater}\right)/w_{dried-sample} = (w_{moist-sample} - w_{dried-sample})/w_{dried-sample} * 100\,[=]\,\% \tag{1}$$

where $w_{evaporatedwater}$, $w_{moist-sample}$, $and w_{dried-sample}$ are the weight of the evaporated water, of the moist and dried sample (g), respectively.

In order to directly reflect the relative change of phenol in the kaolin, all the results are evaluated in terms of normalized phenol concentration C_{Phenol}/C^0_{Phenol} as the ratio of the final phenol content (C_{Phenol}/mg_{Phenol}/Kg of dried kaolin) to the initial content (C^0_{Phenol}/ mg_{Phenol}/Kg of dried kaolin). To check the phenol homogeneity distribution along the cell, the initial phenol content in the kaolin was determined for each experiment at the zero time by sampling approximately 1.00 ± 0.05 g of contaminated kaolin from each region S1, S2 and S3 and analyzing them as previous described. In all the case, the initial concentration of phenol was close to the fixed value of 200 mg_{Phenol}/Kg with a deviation of ±10 mg_{Phenol}/Kg ($C_{Phenol}/C^0_{Phenol} = 1 \pm 0.05$).

The total removal efficiency of phenol, R, refers to the residual phenol at the end of the treatment in all the treated spiked kaolin respect to the initial amount of phenol charged in the cell and was computed by Eq. (2).

$$R = (w^0_{Phenol} - w^{kaolin}_{Phenol})/w^0_{Phenol} * 100 = \sum_{n=S1,S2,S3} (1 - C_{Phenol}/C^0_{Phenol})|_n/3 * 100[=]\% \tag{2}$$

where w^0_{Phenol} is the initial phenol (mg) and w^{kaolin}_{Phenol} is the phenol retained in the kaolin after treatment (mg) in all the amount of kaolin charged in the cell.

Energetic consumption (EC) was computed by Eq. (3):

$$EC = \Delta V * I * t/w * 10^{-3}\,[=]\ \text{kWh/Kg} \tag{3}$$

where ΔV is the applied cell potential (V), I the intensity current (A), t treatment time (s) and w is total mass of treated dried kaolin in the experiment (Kg).

For each experiment, different contaminated kaolin samples (at least two samples of 1.00 ± 0.05 g each) were taken from each section S1, S2 and S3 of the cell and analyzed for the quantification of the phenol content, water content (W), and pH. W of the kaolin samples was determined also at the end of the test in order to evaluate the residual C_{Phenol} expressed as the amount of phenol (mg_{Phenol}) with respect to the dried kaolin (Kg), since, under an applied E, there is a movement of the water from the region close to the anode (S1) towards the cathode side (S3) which slightly change the final water content with respect the initial value. All the analyses were performed in triplicate, and the results were calculated as the average.

After the electrochemical treatment tests were completed, a mass balance was conducted for the phenol in the cell. Over the periods of 4 days, 92%–96% of the initial phenol was recovered, which was considered sufficient for the purposes of this study. These showed that there was an overall mass balance of phenol before and after the test. The discrepancies in the mass balance might be caused by volatilization of phenol and by adsorption to the electrokinetic equipment, such as the Plexiglas cells, electrodes, and sample vials.

3. Results and discussion

3.1. Electrochemical remediation of phenol under direct electric fields

To investigate the effect of a low-strength electric field (E) on the ER of kaolin contaminated by phenol (C^0_{Phenol} of 200 mg/Kg, W of 66%wt.), a first series of electrolyses was performed under a low direct E of 0.25 V cm^{-1} using compact graphite as electrodes for 24, 60 and 96 h. Electrodes were placed in direct contact to the kaolin without any physical barrier to avoid additional electrical resistances. Fig. 2 reports the distribution of the C_{Phenol}/C^0_{Phenol} in the region of the spiked kaolin (S1 — close to the anode area, S2 — middle area, and S3 — close to the cathode area) and the total removal

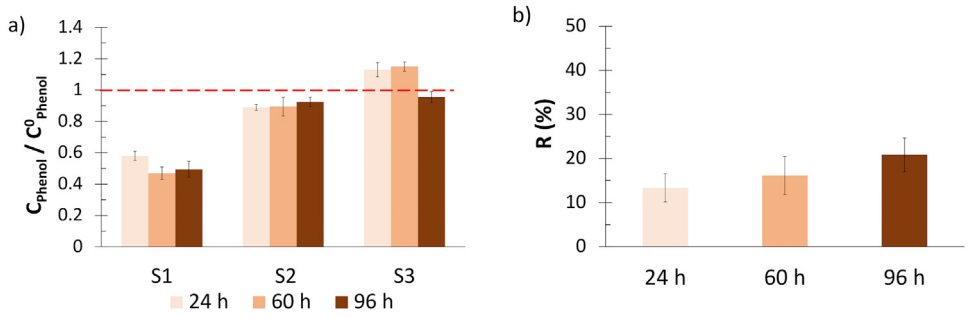

Fig. 2. Effect of the time on the electrokinetic treatment of kaolin contaminated by phenol (C^0_{Phenol} = 200 mg/Kg). *(a)* Plot of the C_{Phenol}/C^0_{Phenol} vs. S1, S2 and S3, which are the sampling position near to the anode, middle and cathode region (as described in detail in the *Section* 2.2), respectively. C_{Phenol}/C^0_{Phenol} of 1 indicates the time zero of treatment: red dashed line (— — —). (*b*) Plot of the total phenol removal, R, vs. time. Electrolyses was performed at 0.25 V cm^{-1} for 24, 60 and 96 h. Compact graphite was used as anode and cathode material. Approximately 66 g of spiked kaolin with a W of 66%wt. was treated in System I.

of phenol from the kaolin. Previous work reported that the kaolin absorption capacity of phenol ranged from 300 (Safwat et al., 2019) to 1000 mg$_{Phenol}$/Kg (Acar et al., 1992); according to Acar et al. (1992) at phenol concentration lower than this range, a most of the phenol was adsorbed by the kaolinite, and its removal required the desorption into the pore fluid and migration towards the electrode. In our work, the initial content of phenol was approximately 200 mg$_{Phenol}$/Kg, which was less than the saturated sorption amount. Hence, also in our case, the mobilization of the phenol requires its desorption from kaolin's particle surface since most of the phenol is expected to be absorbed at this content (Acar et al., 1992). At the beginning of the treatment, the phenol in the spiked kaolin was uniformly distributed (C_{Phenol}/C^0_{Phenol} ~1). After 24 h, under a constant *E* of 0.25 V cm^{-1}, the phenol was concentrated in a specific region of the kaolin (Fig. 2a). In particular, the concentration of phenol was approximately 13% higher with respect to the initial value in the region S3 ($C_{Phenol}/C^0_{Phenol} > 1$) and 10% and 40% lower in the region S2 and S1 ($C_{Phenol}/C^0_{Phenol} < 1$), suggesting that a certain amount of phenol is moved from the region S1 to S3 and it is accumulated in region S3. This result shows that under the low applied *E*, phenol can be desorbed and moved through the kaolin. In particular, the higher content of phenol close to the cathode region (Fig. 2a) indicates that phenol is transported, in our case, by the electroosmotic flow induced in the kaolin from the applied *E* with respect to electromigration mechanism.

When an *E* is applied to a wet low permeability mineral through electrodes, electrolysis of pore fluid occurs at the electrode; using deionized water as electrolyte, the only dominant reaction is the electrolysis of water. Water oxidation produces H^+ at the anode while water reduction generates OH^- at the cathode, resulting in a change of the kaolin pH (Saichek and Reddy, 2003). The change in pH can affect the sorption and dissociation of organics in minerals. In our case, the initial pH of the kaolin was estimated to be approximately 6; in line with the literature, after 96 h, the pH decreased to 3.5 in the region S1 and increased to 8 in the region S3 (see Supplementary Information, CG/CG of Figure S1). Under the adopted conditions, the pH change can be tentatively attributed to the water electrolysis since the applied cell potential (2.5 V) is theoretically sufficient to activate the water electrolysis. The final pH of the contaminated kaolin confirm that phenol is transported through the kaolin via electroosmotic flow, since the pKa of the phenol is 9.98 and at lower pH the phenol is not dissociated to phenolic ions. Hence according to this consideration, other mechanisms, such as electromigration, cannot be considered the main transport mechanism.

In addition, it was found that the phenol was also removed from the kaolin; the total phenol removal after 24 h was approximately of 13% (Fig. 2b); when the treatment was prolonged for 60 and 96 h, a slightly enhancement of the phenol removal up to 16 and 21%, respectively, was observed (Fig. 2b). Thus, it is plausible to suggest that in addition to the mechanical removal of phenol (movement), other mechanisms for the chemical degradation of phenol were involved in the system under a low direct *E* of 0.25 V cm^{-1}. In particular, the removal of phenol can potentially occur at the anode, by anodic oxidation of phenol, and in the kaolin particles. Indeed, according to the literature, during the ER treatment at this very low electric field, the clay particles can act as microelectrodes and several chemical radicals (e.g., reactive oxygen species ROS) on the kaolin particles surfaces are expected to be generated in situ.

It is relevant to highlight that the removal of phenol from kaolin might result also from volatilization. Over the treatment time of 96 h, an almost constant current density of 0.100 ± 0.015 mA cm^{-2} was observed; under such a low *E* and treatment time, kaolin temperature fluctuation can be neglected (Luo et al., 2006; Baraud et al., 1999). However, a control test was also done without the application of current, and no significant changes in phenol concentration and kaolin water content (less than 4%) were observed after 96 h. Hence, it is plausible to confirm that in our approach the removal of phenol due to the volatilization could be neglected.

These findings demonstrated that the electrokinetic remediation of kaolin contaminated by phenol under very low strength *E* of 0.25 V cm^{-1} could be a suitable way to simultaneously desorb, mobilize and in-situ degrade phenol from kaolin. To optimize the process, a series of experiments was carried out with the aim to find the best operative conditions that allow to reach high total phenol removal.

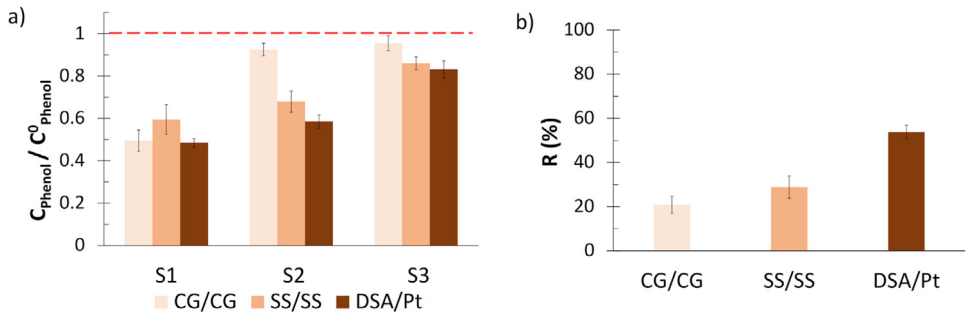

Fig. 3. Effect of the nature of the electrode materials on the electrokinetic treatment of kaolin contaminated by phenol (C^0_{Phenol} = 200 mg/Kg). (*a*) Plot of the C_{Phenol}/C^0_{Phenol} vs. S1, S2 and S3, which are the sampling position near to the anode, middle and cathode region (as described in detail in *Section* 2.2), respectively, after 96 h. C_{Phenol}/C^0_{Phenol} of 1 indicates the time zero of treatment: red dashed line (— — —). (*b*) Comparison of the effect of the electrodes' nature on the total phenol removal, R, after 96 h. Electrolyses was performed under direct *E* of 0.25 V cm^{-1}. Compact graphite (CG/CG), stainless steel electrodes (SS/SS) and DSA® and Platinum (DSA®/Pt) were used as anode and cathode, respectively. Approximately 66 g of spiked kaolin with a W of 66%wt was treated in System I.

3.1.1. *Effect of the nature of electrodes and electric field strength*

The existing research shows that the nature of electrode material can significantly affect the removal efficiency of pollutants during EK process (Gómez et al., 2009; Li et al., 2021; Méndez et al., 2012; Vázquez et al., 2004; Wang et al., 2007; Xiao and Zhou, 2019). It is important to select a good electrode material, according the thermodynamic and kinetic reactions carried out on their surfaces, that should ideally resist to the deposition of insoluble species as well as to corrosion to increase its service life and to reduce the operating costs (Vocciante et al., 2021). According to these considerations, a series of ER under a low strength direct *E* (0.25 V cm^{-1}) was envisioned by testing other two pairs of electrodes in addition to the compact graphite (CG/CG): stainless steel/stainless steel (SS/SS) and Ti/IrO_2-Ta_2O_5 sheet/platinum plate (DSA®/Pt), which were used as anode and cathode (anode/cathode), respectively. ER treatments were carried out for 96 h. Fig. 3 reports the effect of the nature of electrode material on the remediation of kaolin polluted by phenol. In the case of SS/SS, a similar phenol distribution in the kaolin of the CG/CG configuration was observed; indeed, the concentration of phenol increases by moving from S1 to S2 and S3 (Fig. 3a) (C_{Phenol}/C^0_{Phenol} of approximately 0.6, 0.7 and 0.9 in S1, S2 and S3, respectively). More in detail, the concentration of phenol was slightly higher in the region S1 and lower in region S2 and S3 with respect the CG/CG system (Fig. 3a), resulting in a higher total phenol removal of approximately 29% (Fig. 3b). However, the usage of stainless steel (which is conductive material with high strength, good toughness, and low cost (Wen et al., 2017)) as anode is prone to corrosion during the process and can release metal ions thus producing secondary pollution problems (Vocciante et al., 2021). To eliminate the passivation phenomenon, increase electrode life and promote the direct oxidation of the organic pollutants, among others, dimensionally stable anodes (DSA®) (often used for wastewater treatment (Hao et al., 2022; Ltaïef A.H et al., 2018; Martínez-Huitle et al., 2015; Scialdone et al., 2021)) have been tested as anode. In the case of DSA®/Pt, the same trend of the phenol distribution and a further reduction of its concentration in each region of the kaolin was observed (C_{Phenol}/C^0_{Phenol} of approximately 0.3, 0.5 and 0.6 in S1, S2 and S3, respectively), thus achieving a high total phenol removal of approximately 55% after 96 h (Fig. 3b). This is likely to be due to the synergetic effect of the radical ions generated in the kaolin particles and the phenol direct oxidation and with OH radicals produced at the anode. According to the literature, at these electrodes water oxidation gives rise to adsorbed hydroxyl radicals (Eq. (4)) which can participate in the oxidation of organic compounds (Eq. (5)) or potentially evolve towards the formation of chemisorbed oxygen (Eq. (6)) or oxygen evolution (Eqs. (7) and (8)) (Martínez-Huitle et al., 2015).

$$MO_x + H_2O \rightarrow MO_x(\bullet OH) + H^+ + e^- \quad (4)$$

$$MO_x(\bullet OH) + Organics - H \rightarrow MO_x + H_2O + \text{oxidation products} \quad (5)$$

$$MO_x(\bullet OH) \rightarrow MO_{x+1} + H^+ + e^- \quad (6)$$

$$MO_{x+1} \rightarrow MO_x + 0.5O_2 \quad (7)$$

$$MO_x(\bullet OH) \rightarrow MO_x + 0.5O_2 + H^+ + e^- \quad (8)$$

Furthermore, the higher phenol removal in the case of DSA®/Pt configuration could be associated to its lower electrical resistance with respect to the other two system (36.1, 21.4 and 15.24 kΩ for SS/SS, CG/CG and DSA®/Pt, respectively), which probably speed up all the involved mechanisms due to the higher conductivity. The higher electrical resistance in the case of SS/SS could be associated to the formation of an oxidative film on the anode surface during the process which cover the active sites (checked by vision inspection at the end of the electrochemical treatment) since, according to the literature, SS anodes suffer of passivation (Vocciante et al., 2021). In addition, it is worth to mention that the electrode

Table 1
Effect of strength of direct *E* on the electrokinetic remediation of kaolin spiked with phenol and comparison with high relative *E*.[a]

Entry	System	Electrolyte	*E*	C_{Phenol}/C^0_{Phenol}			*pH*			*R*	*EC*
			(V cm^{-1})	S1	S2	S3	S1	S2	S3	(%)	(10^{-3} kWh/Kg)
1	I	–	0.25	0.49	0.92	0.96	3.4	5.2	7.8	21[b]	2.43
2	I	–	0.15	0.31	0.71	0.74	3.2	4.8	5.5	41[b]	1.16
3	I	–	0.05	0.47	0.56	0.46	4.1	4.3	4.4	51[b]	0.30
4	II	Deionized water	1.00	0.38	0.36	0.14	3.3	5.3	7.3	70[c]	24.0

[a] C^0_{Phenol} = 200 mg_{phenol}/Kg. Electrolyses were performed by using CG as anode and cathode materials over a 4-day period. Initial C_{Phenol}/C^0_{Phenol} of 1. Initial pH of 6.
[b] 66 g of spiked kaolin with a W of 66%wt was treated.
[c] 100 g of spiked kaolin with a W of 66%wt was treated.

material had a small impact on the kaolin pH (see SI, Figure S1), in line with previous studies (Li et al., 2021). Despite of the good results achieved by using DSA®/Pt (which is probably the best solution in terms of both stability and energy optimization) and SS/SS in terms of phenol removal, the use of graphite electrodes is much more interesting for the applicative scale because it is inexpensive, has good electrical conductivity and does not require complex treatment with respect to the other kind of electrodes (e.g., DSA®/Pt are more expensive materials or SS needs anti-corrosion treatment).

In line with these considerations, the effect of the strength of *E* on the removal of phenol was studied by using compact graphite as electrode materials over 4-day period. It was observed that a reduction of the applied *E* allows to increase the total removal of phenol from the kaolin (Table 1). An enhance of total phenol removal from 21 to 41 and 51% was reached by moving from 0.25 to 0.15 and 0.05 V cm^{-1} (Table 1), respectively. Furthermore, it was observed that the strength of the *E* influenced the kaolin pH (Table 1). According to the literature, the positive effect of the decrease of the *E* can be tentatively attributed to the fact that, at 0.25 V cm^{-1}, the current is likely to be carried in part by the kaolin particles (thus allowing them to act as microelectrodes and to activate redox reactions at the diffuse-double layer interface) and in part in the pore's fluid (Acar et al., 1995). By decreasing the strength of *E*, the contribution of the ionic current in the fluid pore is likely to be reduced in favor of the percentage of the current transported by the particles. This should enhance the impact of redox reactions involved at the diffuse-double layer interface (Zanko et al., 2020), and, as a consequence, increase the production of free radicals' ions on kaolin particles responsible for the in-situ chemical oxidation of phenol. However, it cannot be excluded that the performances of the process can benefit from the more uniform pH observed at low cell potentials (Table 1).

In order to compare this approach under low-strength *E* values with the usual operative conditions of electrokinetic (EK) treatment process, which uses two additional and external compartments, where electrodes and electrolytes are placed (see System II, *Material and methods Section*), spiked kaolin was treated under 1 V cm^{-1} over a period of 4 days, using system II. This value of *E* was selected in line with the common operative conditions reported in the literature for this kind of remediation technologies (EK) and deionized water was used as processing fluid in the electrolyte compartment. In this case, 100 g of spiked kaolin with a moisture of 66%wt was treated. Under the adopted conditions, it was observed that the distribution of the phenol in the regions S1, S2 and S3 (Table 1, entry 4) is opposite to the trends reported using the other approach (Table 1, entries 1–3), after 4 days of treatment. Under 1 V cm^{-1}, the highest normalized concentration of phenol was observed in the region S1 close to the anode compartment (C_{Phenol}/C^0_{Phenol} of 0.38) and the lowest in S3 close to the cathode one (C_{Phenol}/C^0_{Phenol} of 0.14). In addition, aqueous electrolytes present in the external compartments was analyzed. In the anode compartment no phenol was detected, while phenol was detected in the cathode compartment already after 24 h. This results suggest that phenol was desorbed and transported by electroosmosis of pore fluid water under the induce *E* towards the region S1 to S3 and then pass from the spiked kaolin to the cathode compartment. In this case, the total removal of phenol from the spiked kaolin reached approximately 70% (Table 1, entry 4). Although the higher total removal of phenol was observed under 1 V cm^{-1}, this technology suffer of high energetic consumption per kg of dried treated kaolin (compare Table 1, entries 1–4) and the generation of a secondary pollution effluent (electrolyte was reached in phenol), which must be disposed of and treated as dangerous waste effluent, adding an expensive post-treatment cost. Hence, it is possible to conclude that the use of low values of *E* allows to drastically reduces the energy consumption of the treatment.

3.1.2. Effect of the presence of supporting electrolyte

Electrolytes commonly used in EK remediation are deionized water, NaCl, KH_2PO_4, Na_2SO_4, citric acid, acetic acid, HNO_3, NaOH (Song et al., 2018b; Yuan et al., 2013; Yusni and Tanaka, 2015). Generally, during an EK treatment, the addition of some solutes (i.e NaCl, KH_2PO_4, Na_2SO_4, NaOH) to the electrolyte in the soil directly affects the performances of the process (Cong et al., 2005). In this work, to study the influence of the nature of electrolytes on the ER's performance of kaolinite polluted with phenol, aqueous solution of sodium chloride (0.1 M NaCl) or sodium sulphate (0.1 M Na_2SO_4) was used as electrolytes and added homogeneously into the kaolin. The same concentration of Na_2SO_4 and NaCl was selected to ensure the same amount of anions Cl^- and SO_4^{2-} into the spiked-kaolin. ER experiments were performed using graphite electrodes inserted into the kaolin for 96 h under a low direct *E* of 0.15 V cm^{-1} and compared with the

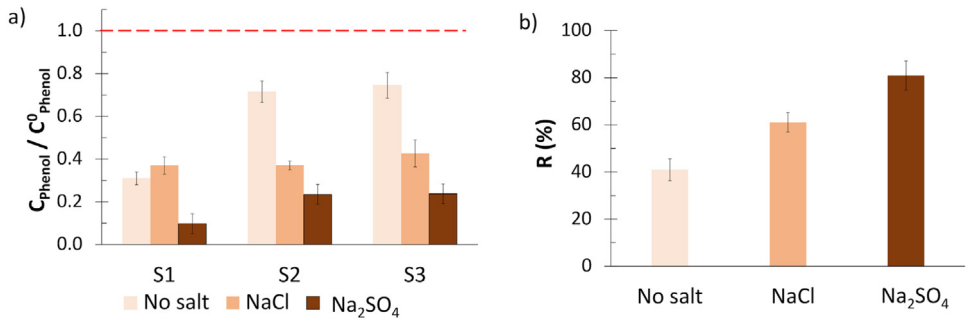

Fig. 4. Effect of the presence of NaCl and Na_2SO_4 in the contaminated kaolin on the electrochemical remediation of phenol (C^0_{Phenol} = 200 mg/Kg). (*a*) Plot of the C_{Phenol}/C^0_{Phenol} vs. S1, S2 and S3, which are the sampling position near to the anode, middle and cathode (as described in detail in *Section* 2.2), respectively. Initial C_{Phenol}/C^0_{Phenol} of 1: red dashed line (— — —). (*b*) Comparison of the total phenol removal, R, after 96 h using distillate water, NaCl and Na_2SO_4 as electrolyte. Electrolyses was performed at 0.15 V cm^{-1} 96 h. Compact graphite (CG/CG) were used as anode and cathode materials, respectively. 66 g of spiked kaolin with a W of 66%wt was treated in System I.

electrolyses performed using water as electrolyte. In the case of NaCl, a constant distribution of phenol concentration in the region S1, S2 and S3 of the kaolinite was observed (C_{Phenol}/C^0_{Phenol} of approximately 0.37, 0.37 and 0.42 in S1, S2 and S3, respectively) (Fig. 4a) coupled with a total phenol removal of approximately 61% (Fig. 4b); thus, showing that the addition of NaCl allows to significantly reduce the content of phenol in the region S1, S2 and S3 and to enhance the phenol removal by approximately 1.5 times with respect to the usage of distillate water (Fig. 4). These results could be rationalized by consider that, in the presence of NaCl and oxidative conditions, active chlorines could be produced at the anode (adsorbed chloro and oxychloro radical) and at the surface of clay particles due the dissociation of NaCl (Eqs. (9)–(11)) (Scialdone et al., 2021) and contribute to the degradation of phenol.

$$2Cl^- \rightarrow Cl_2 + 2e^- \quad (9)$$

$$Cl_{2(aq)} + H_2O \rightarrow HClO + Cl^- + H^+ \quad (10)$$

$$HClO \rightarrow ClO^- + H^+ \quad (11)$$

According to the literature, the relative concentrations of Cl_2, HClO and ClO^- depend on the pH (Cl_2 at pH < 3.0, HClO at 3 ≤ pH ≤ 8 and ClO- at pH > 8) (Scialdone et al., 2021). In the case of NaCl, the final pH values were 5.5, 7.4 and 7.5 in the region S1, S2 and S3, respectively (slightly higher of the distillate water electrolyte) (see SI, Figure S2). On overall, phenol can be oxidized by various oxidants, such as, at the anode surface, adsorbed chloro and oxychloro radicals, and, both at the anode surface and at particles surface, active chlorine, and various other ROS, including HO•, H_2O_2 and $•O_2$, produced by water oxidation.

Furthermore, the addition of a supporting electrolyte allows to slightly increase the conductibility of the kaolin due to the free ions present in the clay, thus increasing the current density and, consequently, speeding up the degradation process (an almost constant current density of 0.057 and 0.068 mA cm^{-2} was observed in absence and in presence of NaCl, respectively).

According to the literature, in presence of Cl^-, it was reported that chlorophenols can be generated (Hao et al., 2022); however, in this work, chlorophenols were not detected at the end of the ER treatment.

When NaCl was replaced with Na_2SO_4, a further reduction of the content of phenol in the polluted kaolinite was observed (Fig. 5a), thus resulting in a higher removal of phenol up to 81% after 96 h (Fig. 5b). To rationalize these results, it is relevant to highlight the work of Choe et al. (2020). These authors proposed a catalytic cycle, wherein hydroxylic radical OH• can migrate to and interact with the SO_4^{2-} functionality to produce, after some steps (Eqs. (12)–(14)), $SO_4•^-$, which decomposes phenol (Eq. (15)). The resulting SO_4^- may accept two electrons to regenerate the SO_4^{2-} functionality (Eq. (16)).

$$OH• + SO_4^{2-} \rightarrow SO_4•^- - {}^-OH \quad (12)$$

$$SO_4•^- - {}^-OH + H^+ \rightarrow SO_4•^- - H_2O \quad (13)$$

$$SO_4•^- - H_2O \rightarrow SO_4•^- + H_2O \quad (14)$$

$$SO_4•^- + \text{phenol} \rightarrow \text{mineralization} + SO_4^- \quad (15)$$

$$SO_4^- + 2e- \rightarrow SO_4^{2-} \quad (16)$$

According to these hypotheses, the highest performances in presence of Na_2SO_4 can be due to the formation *in-situ* of $SO_4•^-$ which is characterized by an enlarged lifetime and strong oxidation potential along with selective oxidation of pollutants, all of which are better than those of OH• (~30 μs and 2.5–3.1 eV for $SO_4•^-$; ~10^{-3} μs and ~2.7 eV for OH•).

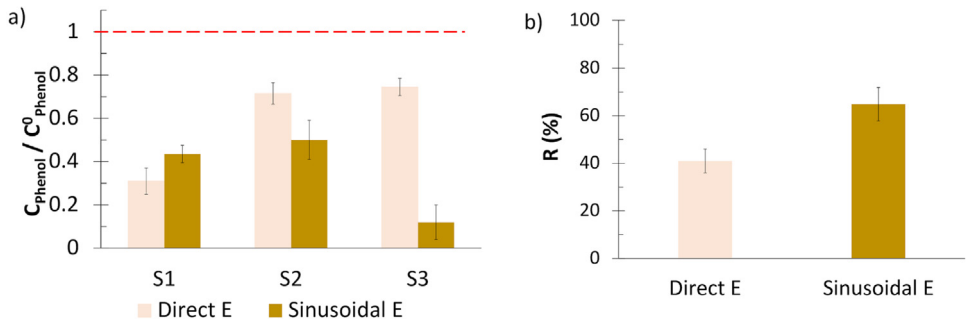

Fig. 5. Comparison of the applied *E* on the electrochemical remediation of kaolin contaminated by phenol over 4 days period: direct or sinusoidal electric field. (a) Plot of the C_{Phenol}/C^0_{Phenol} vs. S1, S2 and S3, which are the sampling position near to the anode, middle and cathode (as described in detail in *Section* 2.2), respectively. Initial C_{Phenol}/C^0_{Phenol} of 1: red dashed line (— — —). Electrolyses was performed under a sinusoidal *E* (direct *E* of 0.15 V cm^{-1} coupled with a sinusoidal *E* of 0.005 ÷ 0.25 V cm^{-1} and *f* 20 Hz). Compact graphite (CG/CG) were used as anode and cathode materials, respectively. Approximately 66 g of spiked kaolin with a W of 66%wt was treated in System I Direct *E* data reflect the results reported in Table 1, entry 2. Sinusoidal *E* data reflect the results reported in Table 2, entry 6.

Also, in the case of Na_2SO_4 a higher current density (0.070 mA cm^{-2}) was recorded with respect to the test in absence of supporting electrolyte, but similar with the one using NaCl, due to the higher conductivity of the contaminated kaolin.

In addition, according to Choe et al. (2020), the formation of persulfates from SO_4^{2-} is favored in acid media conditions due to the role of H^+. In this case, lower pH values of the contaminated kaolinite were observed at the end of the treatment with respect to the other conditions previously reported (see SI, Figure S2); in detail, the pH values were approximately 3.2, 4.7 and 5.5 in region S1, S2 and S3, respectively.

It is relevant to note that under these conditions, chlorinated or persulfates oxidants, which seem to contribute to the phenol degradation, were in situ generated from cheap and non-toxic sources, limiting the operative costs, and improving the sustainability of the process at applicative scale.

3.2. Electrochemical remediation of phenol under sinusoidal electric field

According to the literature, the type of the applied *E* can strongly affect the performances of the process. Some authors have assumed that when, an alternate current is used, the diffuse-double layer acts as capacitor which charges and discharges electricity at the frequency of the alternating current, thus amplifying the electric discharges of the double layer (Zanko et al., 2020). Here, a series of experiments was performed with the aim to investigate the effect of the usage of a direct *E* coupled with a sinusoidal *E* on the performances of the ER of the contaminated kaolin with phenol using compact graphite as electrode materials. Table 2 reports the distribution of the normalized concentration of phenol into kaolin sections and the total phenol removal at the end of the ER. First experiments were performed for 24 h (Table 2, entries 1, 3, 5 and 7). It was shown that the usage a sinusoidal *E*, under all the adopted conditions, allows to reduce the concentration of phenol (C_{Phenol}/C^0_{Phenol} < 1 in all the cases, Table 2, entries 1, 3, 5 and 7) coupled with a total phenol removal higher that 25% in each case after only 24 h. Thus, under all the adopted conditions, the usage of a sinusoidal *E* can be a viable way for the ER of contaminated kaolin. In a second stage, to increase the performance of the process, some selected experiments were performed for 4 days (96 h) (Table 2, entries 2, 4 and 6). It was observed that an increase of the treatment time allows to reduce the C_{Phenol}/C^0_{Phenol} and consequently to enhance the total phenol removal in each case (Table 2, entries 1 and 2, entries 3 and 4, entries 5 and 6). The total phenol removal was enhanced from approximately 37 to 65% after 24 and 96 h, respectively, under a direct *E* of 0.15 V cm^{-1} coupled with a sinusoidal *E* of 0.005 ÷ 0.25 Vcm^{-1} at a frequency (*f*) of 20 Hz (Table 2, entries 5 and 6). These results suggest that, in the case of sinusoidal *E*, the decomposition mechanisms are the same involved when only direct *E* was used, but the usage of sinusoidal *E* allows to speed up the process. In the current literature, up to our knowledge, this effect is not investigated in-depth for the remediation of contaminated minerals, however, it was demonstrated the usage of a sinusoidal *E* allows for acceleration of the remediation performance of the electrokinetic-phytoremediation process with respect to a constant direct *E*. An example given the work of Xu et al. (2020). According to this work, the highest accumulation of Cd by Solanum nigrum L. was observed under AC *E*, which was a very important reference for the electrokinetic condition (Xu et al., 2020).

According to these promising results, the effect of the nature of supporting electrolyte under a sinusoidal *E* was also investigated using NaCl and Na_2SO_4. Electrolyses were performed under direct *E* of 0.15 V cm^{-1} coupled with a sinusoidal *E* of 0.05 ÷ 0.25 V cm^{-1} *f*: 20 Hz for 96 h using compact graphite as electrode materials. In both cases, the addition of a supporting electrolyte gave rise to a lower concentration of phenol in the kaolin coupled with a higher phenol removal (Table 2, entries 2, 8 and 9). The total phenol removal was enhanced from 48 to 56% by adding NaCl into the kaolin (Table 2, entries 2 and 8). Furthermore, the usage of Na_2SO_4 coupled with a sinusoidal *E* allowed to reach a total phenol removal of approximately 90% (Table 2, entry 9). This effect could be rationalized by assuming that the presence of a sinusoidal *E* allows to accelerate the overall process (Eqs. (10)–(14)).

Table 2
Effect of the direct E coupled with a sinusoidal E on the ER of kaolin contaminate by phenol.[a]

Entry	Direct E (V cm^{-1})	Sinusoidal E	Supporting electrolyte	Time (h)	C_{Phenol}/C^0_{Phenol} S1	S2	S3	R (%)
1	0.15	0.05 ÷ 0.25 V cm^{-1} f: 20 Hz	–	24	0.69	0.76	0.69	28.3
2	0.15	0.05 ÷ 0.25 V cm^{-1} f: 20 Hz	–	96	0.61	0.58	0.35	48.5
3	0.15	0.05 ÷ 0.25 V cm^{-1} f: 30 Hz	–	24	0.69	0.71	0.72	29.3
4	0.15	0.05 ÷ 0.25 V cm^{-1} f: 30 Hz	–	96	0.68	0.68	0.45	39.7
5	0.15	0.005 ÷ 0.25 V cm^{-1} f: 20 Hz	–	24	0.79	0.62	0.48	36.8
6	0.15	0.005 ÷ 0.25 V cm^{-1} f: 20 Hz	–	96	0.44	0.50	0.12	64.8
7	0.15	0.005 ÷ 0.25 V cm^{-1} f: 30 Hz	–	24	0.67	0.77	0.77	26.4
8	0.15	0.05 ÷ 0.25 V cm^{-1} f: 20 Hz	NaCl	96	0.45	0.48	0.37	56.2
9	0.15	0.05 ÷ 0.25 V cm^{-1} f: 20 Hz	Na_2SO_4	96	0.06	0.11	0.12	90.6

[a] C^0_{Phenol} = 200 mg$_{phenol}$/Kg. Electrolyses were performed by using CG as electrode materials. Initial $C_{Phenol}/C^0_{tPhenol}$of 1. 66 g of spiked kaolin with a W of 66%wt was used.

In order to directly compare the effect of the type of E on the performances of the ER of contaminated kaolin, Fig. 5 reports the results achieved by performing the ER under direct E of 0.15 V cm^{-1} (Table 1, entry 2) and a direct E of 0.15 V cm^{-1} coupled with a sinusoidal E of 0.005 ÷ 0.25 V cm^{-1} at a frequency (f) of 20 Hz (Table 2, entry 6) using compact graphite as electrode materials for 96 h. In the case of sinusoidal E, the normalized concentration of phenol in the kaolin was higher in the section S1 and lower in S3 (C_{Phenol}/C^0_{Phenol} of approximately 0.44, 0.50 and 0.12 in S1, S2 and S3, respectively) (Fig. 5a), showing an opposite trend to the distribution of phenol observed under only a direct E of 0.15 V cm^{-1}. Moreover, under the adopted conditions, the total removal of phenol was improved of approximately 1.6 times with respect to the results achieved with direct E (41 vs. 64.8% under direct E and sinusoidal E, respectively, Fig. 5b). As already mentioned in previous sections, when E is applied to wet low permeability clay through inert electrodes, electrolysis of pore fluid occurs at the electrodes: oxidation at the anode generates an acid front while reduction at the cathode generates a base front. These acids and bases will advance through clay matrix and change the pH. The change in kaolin pH will affect the sorption and dissociation of organics in particles and will exert significant impact on the efficiency of electrokinetic treatment. Therefore, pH control is of significance for electrokinetic treatment. In the case of a sinusoidal E, the kaolin pH did not appreciable change ranging between 5.6 and 6.2 (see SI, Figure S3); indeed, in the literature it was reported that the usage of alternative current does not provoke pH soil changes (Acosta-Santoyo et al., 2017; Xu et al., 2020). Thus, this route can be a simpler solution under in situ condition with respect to the common strategies reported in the literature, including the usage of conditioning agents or the reactor modifications, to control the pH. According with these results, it is plausible to say that the usage of the sinusoidal E allows to accelerate each single stage of the remediation process.

Finally, the relevant results reached in this work were compared with corresponding literature data reported for electrochemical remediation of low permeability matrix contaminated by phenol (Table 3). Overall, the usage of low-strength E values (see ECGO approach, Table 3, entries 11 and 12) allows to reach good removal efficiencies of phenol, desorbing, mobilizing, also, degrading the phenol in-situ, without the generation of a secondary pollution liquid (expensive post-treatment cost) and at lower energetic consumption.

4. Conclusions

In this work, the electrochemical remediation of contaminated kaolin was investigated using very low values of electric field ($E \leq 0.25$ V cm^{-1}) at the lab-scale. Phenol (200 mg$_{Phenol}$/Kg of dried kaolin) was selected as model hazardous organic compound and kaolin as model low permeability clay. The effect of several factors on the performance of the process was investigated and discussed in terms of the normalized phenol concentration (C_{Phenol}/C^0_{Phenol}) and its total removal from the kaolin.

Overall, the main finding is that the used approach can desorb, mobilize and, in addition to the common findings reported in the literature, degrade the phenol by applying very low values of E, drastically reducing the energy consumption of the treatment and without the generation of a secondary pollution liquid (due to the movement of the phenol from the clay to a liquid phase), which must be disposed of and treated as dangerous waste effluent, adding an expensive post-treatment cost.

More in detail, it was found that:

Table 3
Comparison of electrochemical approaches for the remediation of low permeability matrix spiked by phenolic compounds.

Entry	matrix	Approach[a]	Contaminant	E (V cm^{-1})	Electrodes	Time	C^0_{Phenol} (mg/Kg)	R (%)	References
1	Kaolin	EK	Phenol	2.4–0.7	Graphite	~ 6 days		85–95	Acar et al. (1992)
2	Sandy loam	EK	Phenol	1	Graphite	10 days	165	Only mobilization	Luo et al. (2005)
3	Sandy loam	in-situ-bio-EK with polarity reversal	Phenol	1	Graphite	10 days	180	58	Luo et al. (2006)
4	Sandy loam	EK	Phenol	1	Graphite	6 days	200	<3* only mobilization	Zhang et al. (2005)
5	Kaolin	EK enhanced with the addition of permanganate	Phenol	1	Graphite	5 days	1000	90	Thepsithar and Roberts (2006)
7	Original soil (35% Sand, 65% Clay)	EK	Phenol and chlorophenols	12	Graphite	140 min	1000 mg/L	>70	Cong et al. (2005)
9	Kaolin (high cation clay)	EK	Phenol	1–1.5	Stainless steel	2 days	950	20	Shariatmadari and Falamaki (2007)
10	Kaolin	EK	Phenol	1	Graphite	4 days	200	70	This work
11	Kaolin	ECGO in presence of Na_2SO_4	Phenol	0.15	Graphite	4 days	200	80	This work
12	Kaolin	ECGO in presence of Na_2SO_4	Phenol	0.05 ÷ 0.25 V cm^{-1} f: 20 Hz	Graphite	4 days	200	90	This work

[a]Deionized water was used as processing fluid.
*Evaluated by the authors according to the data contains in the related paper.

- the higher the treatment time, the higher the phenol removal. For example, an increase of the treatment time from 24 to 96 h allows almost double the phenol removal under 0.25 V cm^{-1};
- the efficiency of the process strongly depends on the nature of the electrode: the highest performance in terms of phenol removal was reached by using Pt/DSA® electrodes (~55% phenol removal) with respect to the usage of compact graphite (~20% phenol removal) or stainless steel (~30% phenol removal) electrodes under 0.25 V cm^{-1};
- the usage of the sinusoidal E allows to accelerate each single stage of the remediation process under all the adopted conditions; for example, the total removal of phenol under sinusoidal E was improved by approximately 1.6 times with respect to the results achieved with direct E (41 vs. 64.8% under direct E (0.15 V cm^{-1}) and sinusoidal E (0.005 ÷ 0.25 V cm^{-1} and f 20 Hz), respectively);
- the addition of a suitable supporting electrolyte could drastically affect the process performances by using both a direct and a sinusoidal E. The highest removals of phenol up to approximately 80% and 90% from the kaolin under both direct and sinusoidal E, respectively, were reached using compact graphite as electrodes in presence of Na_2SO_4 in the kaolin.

CRediT authorship contribution statement

Federica Proietto: Investigation, Methodology, Data curation, Conceptualization, Visualization, Writing – original draft, Writing – review & editing. **Abdo Khalil:** Investigation, Data curation. **Wissam Maouch:** Investigation, Data curation. **Alessandro Galia:** Writing – review & editing, Funding acquisition. **Onofrio Scialdone:** Writing – review & editing, Supervision, Funding acquisition.

Declaration of competing interest

The authors declare that they have no known competing financial interests or personal relationships that could have appeared to influence the work reported in this paper.

Data availability

Data will be made available on request.

Acknowledgments

University of Palermo is gratefully acknowledged for the financial support (FFR - Proietto 2023).

Appendix A. Supplementary data

Supplementary material related to this article can be found online at https://doi.org/10.1016/j.eti.2023.103286.

References

Acar, Y.B., Alshawabkeh, A.N., 1993. Principles of electrokinetic remediation. Environ. Sci. Technol. 27, 2638–2647. http://dx.doi.org/10.1021/es00049a002.

Acar, Y.B., Gale, R.J., Alshawabkeh, A.N., Marks, R.E., Puppala, S., Bricka, M., Parker, R., 1995. Electrokinetic remediation: basics and technology status. J. Hazard. Mater. 40 (2), 117–137. http://dx.doi.org/10.1016/0304-3894(94)00066-P.

Acar, Y.B., Li, H., Gale, R.J., 1992. Phenol removal from kaolinite by electrokinetics. J. Geotech. Eng. 118, 1837–1852. http://dx.doi.org/10.1061/(ASCE)0733-9410(1992)118:11(1837).

Acosta-Santoyo, G., Cameselle, C., Bustos, E., 2017. Electrokinetic – Enhanced ryegrass cultures in soils polluted with organic and inorganic compounds. Environ. Res. 158, 118–125. http://dx.doi.org/10.1016/j.envres.2017.06.004.

Al-Shahrani, S.S., Roberts, E.P.L., 2005. Electrokinetic removal of caesium from kaolin. J. Hazard. Mater. B 122, 91–101. http://dx.doi.org/10.1016/j.jhazmat.2005.03.018.

Annamalai, S., Septian, A., Choi, J., Shin, W.S., 2022. Remediation of phenol contaminated soil using persulfate activated by ball-milled colloidal activated carbon. J. Environ. Manag. 310, 114709. http://dx.doi.org/10.1016/j.jenvman.2022.114709.

Baraud, F., Tellier, S., Astruc, M., 1999. Temperature effect on ionic transport during soil electrokinetic treatment at constant pH. J. Hazard. Mater. 64, 263–281. http://dx.doi.org/10.1016/S0304-3894(98)00190-3.

Chen, X., Li, X., Li, Y., Zhao, L., Sun, Y., Rushimisha, I.E., Han, T., Weng, L., Lin, X., Li, Y., 2021. Bioelectric field drives ion migration with the electricity generation and pollutant removal. Environ. Technol. Innov. 24, 101901. http://dx.doi.org/10.1016/j.eti.2021.101901.

Chen, W., Xie, T., Li, W., Wang, R., 2018. Thinking of construction of soil pollution prevention and control technology system in China. Acta Pedol. Sin. 55, 557–568. http://dx.doi.org/10.11766/trxb201711300488.

Choe, Y.J., Kim, J.-S., Kim, H., Kim, J., 2020. Open Ni site coupled with SO_4^{2-} functionality to prompt the radical interconversion of •oh ↔ so_4• $^-$ exploited to decompose refractory pollutants. Chem. Eng. J. 400, 125971. http://dx.doi.org/10.1016/j.cej.2020.125971.

Cong, Y., Ye, Q., Wu, Z., 2005. Electrokinetic behaviour of chlorinated phenols in soil and their electrochemical degradation. Process Saf. Environ. Prot. 83 (B2), 178–183. http://dx.doi.org/10.1205/Psep.03395.

Gereslassie, T., Workineh, A., Atieno, O.J., Wang, J., 2019. Determination of occurrences, distribution, health impacts of organochlorine pesticides in soils of central China. Int. J. Environ. Res. Public Health 16, 146. http://dx.doi.org/10.3390/ijerph16010146.

Gómez, J., Alcántara, M.T., Pazos, M., Sanromán, M.A., 2009. A two-stage process using electrokinetic remediation and electrochemical degradation for treating benzo[a]pyrene spiked kaolin. Chemosphere 74, 1516–1521. http://dx.doi.org/10.1016/j.chemosphere.2008.11.019.

Hao, Y., Ma, H., Proietto, F., Galia, A., Scialdone, O., 2022. Electrochemical treatment of wastewater contaminated by organics and containing chlorides: Effect of operative parameters on the abatement of organics and the generation of chlorinated by-products. Electrochim. Acta 402, 139480. http://dx.doi.org/10.1016/j.electacta.2021.139480.

Hsueh, Y.-S., Chen, X., Dai, Y.-D., Yuan, C., 2022. Comparison of cr/Ni removal by electrokinetic (EK) and electrochemical geooxidation (ECGO) processes: remediation performance and economic analysis in an in-situ system. J. Environ. Chem. Eng. 10, 107018. http://dx.doi.org/10.1016/j.jece.2021.107018.

Huang, D.-Y., Zhou, S.-G., Chen, Q., Zhao, B., Yuan, Y., Zhuang, L., 2011. Enhanced anaerobic degradation of organic pollutants in a soil microbial fuel cell. Chem. Eng. J. 172, 647–653. http://dx.doi.org/10.1016/j.cej.2011.06.024.

Huysegoms, L., Cappuyns, V., 2017. Critical review of decision support tools for sustainability assessment of site remediation options. J. Environ. Manag. 196, 278–296. http://dx.doi.org/10.1016/j.jenvman.2017.03.002.

Karim, A.V., Jiao, Y., Zhou, M., Nidheesh, P.V., 2021. Iron-based persulfate activation process for environmental decontamination in water and soil. Chemosphere 265, 129057. http://dx.doi.org/10.1016/j.chemosphere.2020.129057.

Li, G., Chen, C., Liu, J., Zhang, Y., Li, S., 2021. Effect of soil density and electrode material on the electrokinetic removal of Pb(II) from contaminated silt soil. Int. J. Electrochem. Sci. 16, 211120. http://dx.doi.org/10.20964/2021.11.26.

Li, X., Wang, X., Weng, L., Zhou, Q., Li, Y., 2017. Microbial fuel cell for organic contaminated soil remedial application: A review. Energy Technol. 5, 1156–1164. http://dx.doi.org/10.1002/ente.201600674.

Lin, X., Yang, X., Hu, Z., Zhang, Y., Wang, J., Zhang, Z., Li, Y., 2021. Highly effective removal of bisphenol a by greigite/persulfate in spiked soil: heterogeneous soil/water system balance and degradation. Chemosphere 280, 130655. http://dx.doi.org/10.1016/j.chemosphere.2021.130655.

Ltaïef A.H, S., Proietto, F., Ammar, S., Gabri, A., Galia, A., Scialdone, O., 2018. Electrochemical treatment of aqueous solutions of organic pollutants by electro-fenton with natural heterogeneous catalysts under pressure using Ti/IrO_2-Ta_2O_5or BDD anodes. Chemosphere 202, 111–118. http://dx.doi.org/10.1016/j.chemosphere.2018.03.061.

Luo, Q., Wang, H., Zhang, X., Fan, X., Qian, Y., 2006. In situ bioelectrokinetic remediation of phenol-contaminated soil by use of an electrode matrix and a rotational operation mode. Chemosphere 64, 415–422. http://dx.doi.org/10.1016/j.chemosphere.2005.11.064.

Luo, Q., Zhang, X., Wang, H., Qian, Y., 2005. The use of non-uniform electrokinetics to enhance in situ bioremediation of phenol-contaminated soil. J. Hazard. Mater. 121, 187–194. http://dx.doi.org/10.1016/j.jhazmat.2005.02.007.

Martínez-Huitle, C.A., Rodrigo, M.A., Sirés, I., Scialdone, O., 2015. Single and coupled electrochemical processes and reactors for the abatement of organic water pollutants: A critical review. Chem. Rev. 115, 13362–13407. http://dx.doi.org/10.1021/acs.chemrev.5b00361.

Méndez, E., Pérez, M., Romero, O., Beltràn, E.D., Castro, S., Corona, J.L., Corona, A., Cuevas, M.C., Bustos, E., 2012. Effects of electrode material on the efficiency of hydrocarbon removal by an electrokinetic remediation process. Electrochim. Acta 86, 148–156. http://dx.doi.org/10.1016/j.electacta.2012.04.042.

Rahner, D., Ludwig, G., Röhrs, J., 2002. Electrochemically induced reactions in soils – a new approach to the in-situ remediation of contaminated soils part 1: the microconductor principle. Electrochim. Acta 47 (9), 1395–1403. http://dx.doi.org/10.1016/S0013-4686(01)00854-4.

Reddy, K.R., Cameselle, C., 2009. Electrochemical Remediation Technologies for Polluted Soils, Sediments and Groundwater. John Wiley & Sons, Hoboken, New Jersey.

Röhrs, J., Ludwig, G., Rahner, D., 2002. Electrochemically induced reactions in soils. a new approach to the in-situ remediation of contaminated soils. Part 2: remediation experiments with a natural soil containing highly chlorinated hydrocarbons. Electrochim. Acta 47 (9), 1405–1414. http://dx.doi.org/10.1016/S0013-4686(01)00855-6.

Ronchi, S., Salata, S., Arcidiacono, A., Piroli, E., Montanarella, L., 2019. Policy instruments for soil protection among the EU member states: A comparative analysis. Land Use Policy 82, 763–780. http://dx.doi.org/10.1016/j.landusepol.2019.01.017.
Safwat, S.M., Medhat, M., Abdel-Halim, H., 2019. Phenol adsorption onto kaolin and fuller's earth: A comparative study with bentonite. Desalination Water Treat 155, 197–206. http://dx.doi.org/10.5004/dwt.2019.24051.
Saichek, R.E., Reddy, K.R., 2003. Effect of pH control at the anode for the electrokinetic removal of phenanthrene from kaolin soil. Chemosphere 51, 273–287. http://dx.doi.org/10.1016/S0045-6535(02)00849-4.
Saini, A., Bekele, D.N., Chadalavada, S., Fang, C., Naidu, R., 2021. Electrokinetic remediation of petroleum hydrocarbon contaminated soil (I). Environ. Technol. Innov. 23, 101585. http://dx.doi.org/10.1016/j.eti.2021.101585.
Scialdone, O., Proietto, F., Galia, A., 2021. Electrochemical production and use of chlorinated oxidants for the treatment of wastewater contaminated by organic pollutants and disinfection. Curr. Opin. Electrochem. 27, 100682. http://dx.doi.org/10.1016/j.coelec.2020.100682.
Shariatmadari, N., Falamaki, A., 2007. Electrokinetic removal of phenol and petroleum hydrocarbons ffom contaminated clays. Kuwait J. Sci. Eng. 34 (1B), 73–90.
Sharma, H.D., Reddy, K.R., 2004. Geoenvironmental Engineering: Site Remediation, Waste Containment, and Emerging Waste Management Technologies, first ed. John Wiley & Sons, Hoboken, New Jersey.
Soil strategy for 2030, 2023. Official web site of the european union. https://environment.ec.europa.eu/strategy/soil-strategy_en (accessed 16 2023).
Song, Y., Cang, L., Fang, G., Ata-Ul-Karim, S.T., Xu, H., Zhou, D., 2018b. Electrokinetic delivery of anodic in situ generated active chlorine to remediate diesel-contaminated sand. Chem. Eng. J. 337, 499–505. http://dx.doi.org/10.1016/j.cej.2017.12.122.
Song, Y., Hou, D., Zhang, J., O'Connor, D., Li, G., Gu, Q., Li, S., Liu, P., 2018a. Environmental and socio-economic sustainability appraisal of contaminated land remediation strategies: A case study at a mega-site in China. Sci. Total Environ. 610, 391–401. http://dx.doi.org/10.1016/j.scitotenv.2017.08.016.
Tang, J., Qiu, Z., Tang, H., Wang, H., Sima, W., Liang, C., Liao, Y., Li, Z., Wan, S., Dong, J., 2021. Coupled with EDDS and approaching anode technique enhanced electrokinetic remediation removal heavy metal from sludge. Environ. Pollut. 272, 115975. http://dx.doi.org/10.1016/j.envpol.2020.115975.
Thepsithar, P., Roberts, E.P.L., 2006. Removal of phenol from contaminated kaolin using electrokinetically enhanced in situ chemical oxidation. Environ. Sci. Technol. 40, 6098–6103. http://dx.doi.org/10.1021/es060883f.
Vaiano, V., Matarangolo, M., Murcia, J.J., Rojas, H., Navío, J.A., Hidalgo, M.C., 2018. Enhanced photocatalytic removal of phenol from aqueous solutions using ZnO modified with Ag. Appl. Catal. B: Environ. 225, 197–206. http://dx.doi.org/10.1016/j.apcatb.2017.11.075.
Vázquez, M.V., Hernández-Luis, F., Grandoso, D., Arbelo, C.D., 2004. Study of the electrical resistance of and soils subjected to electro-remediation treatment. Port. Electrochimica Acta 22, 399–410. http://dx.doi.org/10.4152/pea.200404399.
Vocciante, M., Dovì, V.G., Ferro, S., 2021. Sustainability in ElectroKinetic remediation processes: A critical analysis. Sustainability 13 (770), http://dx.doi.org/10.3390/su13020770.
Wang, J.Y., Huang, X.-J., Kao, J.C.M., Stabnikova, O., 2007. Simultaneous removal of organic contaminants and heavy metals from kaolin using an upward electrokinetic soil remediation process. J. Hazard. Mater. 144, 292–299. http://dx.doi.org/10.1016/j.jhazmat.2006.10.026.
Wang, J., Wang, S., 2018. Activation of persulfate (PS) and peroxymonosulfate (PMS) and application for the degradation of emerging contaminants. Chem. Eng. J. 334, 1502–1517. http://dx.doi.org/10.1016/j.cej.2017.11.059.
Wen, D.D., Fu, R.B., Zhang, W., Gu, Y.Y., 2017. Enhanced electrokinetic remediation of heavy metals contaminated soils by stainless steel electrodes as well as the phenomenon and mechanism of electrode corrosion and crystallization. Huan Jing Ke Xue 38, 1209–1217. http://dx.doi.org/10.13227/j.hjkx.201608195.
Wu, Y., Jing, W., Gao, C., Huang, Q., Cai, P., 2018. Recent advances in microbial electrochemical system for soil bioremediation. Chemosphere 211, 156–163. http://dx.doi.org/10.1016/j.chemosphere.2018.07.089.
Xiao, J., Zhou, S., 2019. Effect of electrode materials on electro kinetic remediation of uranium contaminated soil. IOP Conf. Ser.: Earth Environ. Sci. 300, 032074. http://dx.doi.org/10.1088/1755-1315/300/3/032074.
Xu, L., Dai, H., Skuza, H.L., Wei, S., 2020. The effects of different electric fields and electrodes on solanum nigrum L. Cd hyperaccumulation in soil. Chemosphere 246, 125666. http://dx.doi.org/10.1016/j.chemosphere.2019.125666.
Yuan, C., Chen, C.-Y., Hung, C.-H., 2013. Electrochemical remediation of BPA in a soil matrix by Pd/Ti and RuO_2/Ti electrodes. J. Appl. Electrochem. 43, 1163–1174. http://dx.doi.org/10.1007/s10800-013-0600-z.
Yusni, E.M., Tanaka, S., 2015. Removal behaviour of a thiazine, an azo and a triarylmethane dyes from polluted kaolinitic soil using electrokinetic remediation technology. Electrochim. Acta 181, 130–138. http://dx.doi.org/10.1016/j.electacta.2015.06.153.
Zanko, L.M., Wittle, J.K., Pamukcu, S., 2020. Case study: electrochemical geo-oxidation (ECGO) treatment of massachusetts new bedford harbor sediment PCBs. Electrochim. Acta 354, 136690. http://dx.doi.org/10.1016/j.electacta.2020.136690.
Zhang, X., Wang, H., Qian, Y., 2005. Mobilization of phenol and dichlorophenol in unsaturated soils by non-uniform electrokinetics. Chemosphere 59, 1289–1298. http://dx.doi.org/10.1016/j.chemosphere.2004.11.043.